Commensal microbiota influence systemic autoimmune responses

Jens T. Van Praet[1,11], Erin Donovan[1,11], Inge Vanassche[1], Michael B. Drennan[1], Amélie Dendooven[2], Liesbeth Allais[3], Claude A. Cuvelier[3], Fons van de Loo[4], Paula S. Norris[5], Sergei A. Nedospasov[6], Sylvie Rabot[7,8], Tom Van de Wiele[9], Gérard Eberl[10], Carl F. Ware[5] and Dirk Elewaut[1,12].

[1]Laboratory for Molecular Immunology and Inflammation, Department of Rheumatology, Ghent University Hospital, Belgium

[2]Department of Pathology, University Medical Center Utrecht, The Netherlands

[3]Department of Pathology, Ghent University Hospital, Belgium

[4]Department of Rheumatology, Radboud University Medical Center, The Netherlands

[5]Infectious and Inflammatory Disease Center, Sanford-Burnham Medical Research Institute, La Jolla, USA

[6]Engelhardt Institute of Molecular Biology, Russian Academy of Sciences, and Lomonosov Moscow State University, 119991 Moscow, Russia

[7]INRA, UMR1319 Micalis, Jouy-en-Josas, France

[8]AgroParisTech, Micalis, Jouy-en-Josas, France

[9]Laboratory of Microbial Ecology and Technology, Ghent University, Belgium

[10]Lymphoid Tissue Development Group, Institut Pasteur, Paris, France

[11]JTVP and ED share equal contribution to this work

[12]Address correspondence to:

Dirk Elewaut, MD, PhD
Department of Rheumatology
University Hospital Ghent, 0K12-IB
De Pintelaan 185
9000 Gent, Belgium
+3293322240
Dirk.Elewaut@ugent.be

Abstract (200 words)

Systemic autoimmune responses are a hallmark feature of generalized autoimmune diseases, including systemic lupus erythematosus (SLE) and systemic sclerosis (SSc)[1]. These clinically heterogeneous conditions are characterised by immune-mediated tissue damage in multiple organs, caused by aberrant responses of the adaptive immune system. However, the processes underlying the loss of tolerance against self constituents is unresolved. The lymphotoxin-β receptor (LTβR) functions as receptor for both membrane-bound lymphotoxin (LTα1β2) and LIGHT (TNF superfamily member 14)[2]. LTβR controls the development of secondary lymphoid organs, and is continuously required in adults for homeostasis and structural architecture of the thymus and secondary lymphoid organs. Using mice deficient in LT and Hox11, we report that approximately 25% of mice lacking secondary lymphoid organs spontaneously develop antinuclear antibodies. Interestingly, this phenotype is not caused by a defect in central tolerance. Rather, cell-specific deletion and *in vivo* LT blockade link these systemic autoimmune responses to gut associated lymphoid tissue in the neonatal period of life. We further demonstrate that autoantibody production is influenced by the presence of commensal gut flora, especially segmented filamentous bacteria, IL-17 receptor signalling and the production of IgA. Together, these data indicate that neonatal colonization of gut microbiota influences generalized autoimmunity in adult life.

Manuscript

Autoantibodies against nuclear antigens are a hallmark feature of generalized autoimmune diseases[1]. Immunodominant autoantigens recognized by systemic autoantibodies are often DNA- or RNA-associated protein complexes. Underlying mechanisms that mediate the breach of tolerance against these autoantigens are only partially understood. In autoimmune-prone strains of mice, antigen-producing cells have been located in secondary lymphoid tissue, and both extrafollicular and germinal centre responses have been implicated in the production of such autoantibodies[3,4].

LT-deficient mice serve as a prototypic model for studying the influence of secondary lymphoid organs in immune processes. Although antibody responses are impaired in LT-deficient animals due to absence of follicular dendritic cell networks, germinal centre formation and somatic hypermutation can still occur[5]. Based on the presence of perivascular lymphocytic infiltrates in multiple organs as well as organ specific autoantibodies an autoimmune phenotype has been defined for the LT-deficient animals[6]. However, the role of the disturbed thymic medulla in this autoimmune phenotype is a matter of controversy[7-9]. Whether systemic autoimmune responses do occur in absence of secondary lymphoid tissues is another area of uncertainty[6,7]. Given conflicting reports on systemic autoimmune responses in *Ltbr*$^{-/-}$ mice, we sought to investigate whether autoantibodies directed against nuclear antigens can appear in absence of secondary lymphoid tissues utilizing *Ltbr*$^{-/-}$ mice.

We found that ~25% of LTβR-deficient mice developed systemic autoimmune responses by three months of age (Fig. 1a) using a validated immunodetection system for a broad range of nuclear antigens (Supplementary Fig. 1). The immunoassay system identified anti-extractable nuclear antigen (ENA) antibodies, including anti-U1RNP, anti-Sm, anti-Scl70/Topoisomerase-I, anti-Centromere protein B, anti-SSA/Ro52 and anti-Jo1 (Fig. 1b and b). Antibodies to these autoantigens are strongly associated with SLE, SSc and polymyositis[1]. In contrast, no anti-dsDNA was found (Supplementary Fig. 2). By six months of age, the prevalence of autoantibodies remained the same, but more mice developed multiple reactivities (Fig. 1b and 1c). We could not detect any autoimmune reactivity at six weeks of age despite immune maturation, suggesting a delayed stochastic penetrance of the autoimmune phenotype characteristic in most autoimmune diseases. As LT-deficient animals have a spleen, we sought to

determine whether autoantibodies can be generated in asplenic mice by intercrossing *Hox-11*$^{-/-}$ and *Ltbr* $^{-/-}$ mice. These double knock-out mice still developed the pathological autoantibody responses at the same prevalence, demonstrating that aberrant systemic autoimmune responses can develop in the complete absence of secondary lymphoid organs (Fig. 1a).

Histological examination of *Ltbr* $^{-/-}$ mice confirmed the presence of lymphocytic infiltrates in multiple organs. Given the association of systemic autoimmune responses with generalised autoimmune disease, we specifically looked for characteristic pathological features. However, compared to wild-type mice, no difference was observed in kidney damage, and skin and oesophageal sclerosis (Supplementary Fig. 3). Furthermore, renal histology and proteinuria were not different between antibody positive and negative *Ltbr* $^{-/-}$ mice (data not shown).

We then evaluated whether structural defects in LT-deficient mice lead to systemic autoimmune responses. To this end, we used an LTβR-Fc fusion protein, which acts as a soluble decoy receptor blocking LTαβ and LIGHT[10]. Blocking LTβR signalling at various phases of ontogeny and early postnatally results in the temporally patterned absence of secondary lymphoid organs (lymph nodes, Peyers' patches (PP) and cryptopathes (CP))[10-12]. We observed that blocking LTβR signalling during late ontogeny through six weeks of age resulted in the appearance of autoantibodies at the age of three months (Fig. 1d), and as demonstrated previously, these mice lacked CP, PP and ILF (data not shown). In contrast, mice lacking peripheral lymph nodes and PP by blocking LTβR signalling during early ontogeny did not develop autoantibodies. In addition, blocking LTβR signalling during adulthood, which disrupts splenic architecture also did not result in autoantibody formation (Fig. 1d). To rule out a role of LTβR signalling in the thymus during the perinatal window, we performed thymus transplant experiments. Fetal thymi from *Ltbr*$^{-/-}$ or wild-type mice were depleted of hematopoietic cells and then grafted under the kidney capsules of nude mice, creating *Ltbr*$^{-/-}$→nude mice and wild-type→nude mice. Twelve weeks after engraftment, mice were sacrificed and T cell repopulation was verified in the liver and spleen by flow cytometry (Supplementary Fig. 4a and 4b). *Ltbr*$^{-/-}$ and wild-type thymi contained approximately equal number of thymocytes, with similar distribution among the different T cell subsets (Supplementary Fig. 4a). Levels of total IgG were also not different between the two groups (Supplementary Fig. 4c). Importantly, no autoantibodies could be detected in the serum samples of nude mice engrafted with LTβR-deficient thymic lobes

(Supplementary Fig. 4d). We thus concluded that systemic autoimmune responses can develop in absence of CP and ILF.

We next wanted to resolve which membrane LT-expressing cell type in the lamina propria of the gut was involved in maintenance of tolerance against nuclear antigens. To this end, we generated mice deficient in LTβ in T cells (T-*Ltb*$^{-/-}$), B cells (B-*Ltb*$^{-/-}$) or RORγt+ cells (Rorγt-*Ltb*$^{-/-}$). We could only detect autoantibodies with a similar spectrum as *Ltbr*$^{-/-}$ in mice lacking membrane LT in RORγt positive cells (Fig. 1e). To resolve which LTβR-expressing cells in the lamina propria are involved in the maintenance of the tolerance, we performed reciprocal bone marrow transfer experiments between wild-type and *Ltbr*$^{-/-}$ mice. As shown in Figure 1f, both wild-type→*Ltbr*$^{-/-}$ and *Ltbr*$^{-/-}$→wild-type chimeras developed autoantibodies. We thus conclude that communication via the LT-LTβR axis between RORγt+ innate lymphoid cells (ILC) and both radio-resistant and bone marrow-derived cells is essential to maintain tolerance.

RORγt+ ILC have been shown to be essential in the defence of epithelial surfaces, and play an important role in the intestinal homeostasis with symbiotic microbiota by the production of IgA, IL-17 and IL-22 production[13]. This regulatory control in the gut prompted us to examine the relationship between the gut microbiota and autoantibody production. Moreover, early postnatal blocking of LTβR signalling leads to a 10-fold expansion of the normal ileal microbiota, including bacteria belonging to the Clostridiales, Bacteroides and Enterobacteriaceae groups[12]. We assessed whether elimination of the gut microbiota influenced autoantibody production. Pregnant mice and their offspring were treated with broad-spectrum antibiotics until the age of 12 weeks. As previously observed in germfree mice, this caused a significant enlargement of the caecum (data not shown). *Ltbr*$^{-/-}$ mice receiving antibiotics had reduced prevalence of autoantibodies compared to untreated animals (Fig. 2a, upper panel). To further substantiate a role for the gut microbiota, we treated germ free C57BL/6 mice with the LTβR-Fc fusion protein from gestational day 18 until six weeks after birth as described above. Similarly, germ free animals had a reduced prevalence of autoantibodies (Fig. 2a, lower panel). We next assessed whether gut microbiota composition differed between wild-type, antibody-positive and -negative LTβR deficient animals existed. In a first screening, we performed a community profiling with denaturing gradient gel electrophoresis (DGGE) on the luminal, mucosal and fecal microbiome. As shown on Figure 2b, we observed genotype and antibody-specific clustering of the three

animal groups. Cloning and sequencing of the gel band that differed most between the groups revealed a species belonging to the segmented filamentous bacteria (SFB), characterizing animals with multiple reactivities as a separate group. These data were confirmed by quantitative PCR with primers specific for SFB genes (Fig. 2c). Histological analyses of different gut parts comparing antibody positive and negative LTβR deficient animals revealed no inflammatory differences (Supplementary Fig. 5 and Supplementary Fig. 6). SFB are important for inducing a robust T-helper cell type 17 population in the small-intestinal lamina propria of the mouse gut[14]. To assess the potential role of IL-17 or IL-25 in the model as an effector cytokine, we treated IL-17R-deficient mice with the LTβR-Fc fusion protein from gestational day 18 until six weeks after birth as described above. In contrast to wild-type mice, this treatment did not induce significant systemic autoimmune responses (Fig. 2d). In BXD2, a mouse model for lupus, IL-17 was also identified as an important effector cytokine for systemic autoimmune responses[15].

ILF and PP contain the stromal micro-environment for IgA production, a critical antibody that helps maintain gut homeostasis[16]. We determined IgA levels in animals with and without multiple autoantibodies. As shown in Figure 3a multiple anti-ENA positive animals had markedly lower serum IgA levels compared to negative animals. A similar reduction of IgA levels, and IgA positive cells in the terminal ileum, was observed in multiple anti-ENA positive mice treated with LTβR-Fc fusion protein (data not shown). In addition, a decrease in IgA but not in IgG levels, was also apparent in human SLE patients, compared to other forms of arthritis lacking antinuclear antibodies such as rheumatoid arthritis or spondyloarthritis (Fig. 3b and 3c). SFB colonization of the small intestine has previously been shown to increase IgA producing B cells[17]. Furthermore, IgA has been implicated in controlling SFB colonization[18]. We report that in the absence of LT IL-17R-dependent systemic autoimmune responses are associated with SFB colonization and decreased IgA levels. Overall, our findings enforce a new paradigm that neonatal colonization of the gut impacts systemic autoimmune responses against nuclear antigens in adulthood by increased colonization of the intestine by SFB.

Acknowledgements

The authors greatly appreciate the technical assistance of F. Windels, T. Decruy, T. Lacoere, S. Maertens, J. Coudenys, N. Degryse and E. Verheugen. This work is supported by a fund of Scientific Research– Flanders (FWO) and by a concerted research action grant of the Research Council of Ghent University. DE is also a member of a multidisciplinary research platform (MRP) of Ghent University and is supported by Interuniversity Attraction Pole (IUAP) grant Devrepair from the Belspo Agency (project P7/07). DE is also supported by from the EU's seventh framework program under EC-GA n° 305266 'MIAMI'.

Author contributions

JTVP, ED and DE conceived of and designed the study. JTVP, ED, IV, MBD, AD, LA, CAC, FvdL, TVdW, PSN, SAN, SR and CFW performed the experiments. JTVP, ED, TVdW, GE and ED analyzed the data. JTVP and DE wrote the manuscript.

Competing financial interests

The authors declare no competing financial interests

Methods

Mice

C57BL/6 and nude mice (C57BL/6 background) were originally purchased from The Jackson Laboratory. Mice deficient in LTα[19] (backcrossed 8 times on C57BL/6), LTβR[20] (backcrossed 6 times), LIGHT[21] (backcrossed 6 times), HOX11[22] (backcrossed 10 times) and IL17R[23] (backcrossed more than 10 times) have been described previously. *Ltb*$^{-/-}$, T-*Ltb*$^{-/-}$, B-*Ltb*$^{-/-}$ and Rorγt-*Ltb*$^{-/-}$ were generated by crossing LTβ-floxed mice[24] with K5-cre[25], CD4-cre[26], mb1-cre[27] and RORγt-cre[28], respectively. MRL/*lpr*$^{-/-}$ and (NZB/NZW)F1 mice were purchased from Harlan Europe. Sera from NOD mice were kindly provided by Prof C. Mathieu (University Hospital Leuven, Belgium). Pristane-induced lupus in C57BL/6 was performed as described previously[29]. Germ free C57BL/6 were obtained from the INRA Anaxem germfree animal facilities (Jouy-en-Josas, France) and housed in isolators. Other mice were housed and bred in a specific pathogen-free facility. All animal procedures were approved by the Institutional Animal Care and Ethics Committee of Ghent University.

Patients

Serum samples for testing IgA and IgG levels were selected from previously described cohorts of patients with systemic lupus erythematosus[30], rheumatoid arthritis[31] and spondyloarthritis[32]. This study was conducted after approval by the ethical committee of the Ghent University Hospital and informed consent was obtained from these patients.

Antibodies, fusion protein, antibiotics and ELISA

Pregnant mice were injected simultaneously i.v. and i.p. with 50 μg of LTβR-Fc on day 11 and day 15 of gestation, or only on day 18 of gestation. When the mother was injected only at day 18, progeny received weekly i.p. injections with 25 μg of LTβR-Fc (continuous) starting at day 7 after birth until the age of 6 weeks. Controls consisted of C57BL/6 mice treated with control IgG. In addition, adult C57BL/6 mice (8 weeks) were injected i.p. weekly with 100 μg of LTβR-Fc or control immunoglobulin for 7 weeks. Ampicillin, streptomycin and colistin (Sigma-Aldrich) were supplied to mice in the drinking water at a concentration of 1 g/l, 5 g/l and 1 g/l, respectively. Murine IgA and human IgA and IgG antibodies were detected with ELISA according to the manufacturer's instructions (eBioscience).

Thymus transplants

Thymi were isolated from newborn *Ltbr*$^{-/-}$ or wild-type mice and cultured in 1.35 mM 2-deoxyguanosine (Sigma-Aldrich) for 5 days to deplete bone marrow-derived cells. Two thymic lobes were then transplanted under the kidney capsule of adult nude mice[9]. Mice were bled 6 weeks after the procedure to verify the presence of circulating T cells by flowcytometry. After 12 weeks mice were bled and sacrificed. Thymic lobes, liver and spleen cells were analyzed by flow cytometry.

Bone marrow transfers

Bone marrow was isolated from the femur and tibia of *Ltbr*$^{-/-}$ or wild-type mice. Three million bone marrow cells were injected in the liver of sublethally-irradiated (400 rad) 7 day-old C57BL/6 and LTβR deficient recipient mice.

Anti-extractable nuclear antigen and anti-dsDNA antibodies

Anti-ENA were detected by line immunoassay (INNO-LIA ANA Update, Innogenetics NV). The nylon strips were incubated with serum at a 1/200 dilution. Following washing, a 1:2500 dilution of an alkaline phosphatase-conjugated anti-mouse IgG was added (Chemicon). After washing, the reaction was revealed with the chromogen 5-bromo-4-chloro-3-indolyl phosphatase, producing a dark brown color in proportion to the amount of specific autoantibody in the test sample. Sulphuric acid was added to stop the color development. The cutoff of the reactivities was determined by testing 20 serum samples from 6-month-old C57BL/6 mice. None produced any background staining higher than a 1:12800 dilution of a strong anti-RNP-A reactivity of a *MRL/lpr*$^{-/-}$ mouse. Thus, we considered a higher intensity as a positive test result. The assay contains the following recombinant and natural antigens: SmB, SmD, RNP-A, RNP-C, RNP-70k, Ro52/SSA, Ro60/SSA, La/SSB, CenpB, Topo-I/Scl70, Jo-1, ribosomal P, and histones. Anti-dsDNA IgG antibodies were detected with ELISA according to the manufacturer's instructions (Alpha Diagnostic International).

Histopathology

Tissues for histological examination were fixed in 4% buffered formaldehyde and embedded in paraffin. Sections were stained with haematoxylin and eosin, periodic-acid Schiff, silver staining and Masson's trichrome using the standard technique. For electron microscopy, intestinal samples were fixed in 0.1 M cacodylate buffer containing 4% paraformaldehyde and 5% glutaraldehyde during 48 h. Then, samples were washed overnight with 0.1 M Sodium cacodylate buffer. Following postfixation in 1% osmium tetroxide for 3 h, samples were dehydrated in a series of alcohol (15' 50%, 15' 70%, 15' 90% and 3 times 30' 100%) and embedded in Epon medium (Aurion). Semithin sections of 1 μm were cut and stained with toluidine blue to select the most appropriate area of the intestinal sample to be visualized. Ultrathin sections of 60 nm were cut and contrasted with uranyl acetate and lead nitrate, followed by imaging with a Zeiss TEM900 transmission electron microscope (Carl Zeiss) at 50 kV. De-identification and coding of slides was done so that a blinded evaluation could be performed. Slides were scored by trained pathologists (LA and CAC, for the gut sections, AD for the renal sections). Renal slides were scored as described previously.[33] Briefly, for glomerular damage, 10 random glomeruli of each animal were scored using a semi-quantitative grading system. In this grading system, a grade 0 corresponds with specimens with no glomerular lesions, grade I lesions show minimal mesangial thickening, grade II lesions contain increases in both mesangium and glomerular cellularity, and grade III lesions contain the preceding features plus superimposed inflammation and/or capsular adhesions. Grade IV lesions show obliteration of glomerular architecture involving more than 70% of the glomeruli. Furthermore, glomerular crescents, interstitial inflammation and vascular inflammation were described. Dermal sclerosis and esophageal sclerosis was determined using ImageJ to measure the thickness of dermis and submucosa. Inflammatory scores of different part of the gut were performed according to an adapted scoring scheme[34] (Supplementary Fig. 5b).

Flow cytometry

Liver mononuclear cells were isolated using an adjusted 33% Percoll gradient (GE Healthcare)[35]. Cell suspensions from thymus and spleen were prepared by conventional methods. Mononuclear cells were isolated from peripheral blood using a Ficoll Paque Plus gradient (GE Healthcare). Cell stainings were performed as described previously[35]. Cells were acquired on a FACSCanto II (Becton Dickinson) flow cytometer and analyzed using FlowJo software (Tree Star). Primary

antibodies used were from eBioscience: anti-TCRβ (H57-597), anti-CD4 (L3T4), anti-CD8 (Ly-2), anti-FOXP3 (FJK-16s) and B220–APC-Cy7.

Analysis of the gut flora

The most prominent shifts within the microbiota were monitored via denaturing gradient gel electrophoresis (DGGE). After DNA extraction[36] and PCR[37], gels were run using an Ingeny PhorU apparatus (Ingeny International). DNA-fragment bands on the DGGE gel that distinguished autoantibody positive from negative samples on the DGGE gel, were identified through sequence analysis. Specific bands were cut from the gel, after which the 180 bp sized fragment were sequenced (AGOWA). Normalization and further analysis of the gels was carried out using BioNumerics software v5.10. To identify the band of interest in more phylogenetic detail, a clone library was made from the samples of interest. PCR was performed on the sample with primers F27/R1492. PCR products were cut from the gel, purified (QIAquick Gel Extraction Kit, QIAGEN) and cloned with a TOPO TA Cloning Kit with PCR2.1- TOPO Vector (Invitrogen). Clone DNA was amplified with primers M13F/M13R, after which nested PCR was followed with DGGE primers GC-338F/518R. Clones from which the DNA band on DGGE matched with the DNA band of interest (distinctive between autoantibody positive and negative) were sent for sequencing (AGOWA). Sequences (480 bp) were manually inspected and compared with databases at the NCBI website (http://blast.ncbi.nlm.nih.gov/blast.cgi). Following the identification of segmented filamentous bacteria (SFB) as distinctive DNA band between autoantibody positive and negative mice, we next performed a quantitative analysis of SFB with qPCR using primers SFB736F and SFB844R as reported previously.[38]

Statistical analysis

For categorical data analyses, Fisher's exact tests were used, whereas continuous data were analyzed by student's t-tests, Mann Withney U tests or ANOVA with Bonferroni *post-hoc* tests, using PASW 18.0 (IBM). Pearson correlation and UPGMA (Unweighted Pair Group Method using Arithmetic Mean) clustering were used to calculate dendrograms, using BioNumerics v5.10 (Applied Maths).

References

1. von Muhlen, C.A. & Tan, E.M. Autoantibodies in the diagnosis of systemic rheumatic diseases. *Semin Arthritis Rheum* **24**, 323-358 (1995).
2. Ware, C.F. Network communications: lymphotoxins, LIGHT, and TNF. *Annu Rev Immunol* **23**, 787-819 (2005).
3. William, J., Euler, C., Christensen, S. & Shlomchik, M.J. Evolution of autoantibody responses via somatic hypermutation outside of germinal centers. *Science* **297**, 2066-2070 (2002).
4. Vinuesa, C.G.*, et al.* A RING-type ubiquitin ligase family member required to repress follicular helper T cells and autoimmunity. *Nature* **435**, 452-458 (2005).
5. Koni, P.A. & Flavell, R.A. Lymph node germinal centers form in the absence of follicular dendritic cell networks. *J Exp Med* **189**, 855-864 (1999).
6. Boehm, T., Scheu, S., Pfeffer, K. & Bleul, C.C. Thymic medullary epithelial cell differentiation, thymocyte emigration, and the control of autoimmunity require lympho-epithelial cross talk via LTbetaR. *J Exp Med* **198**, 757-769 (2003).
7. Chin, R.K.*, et al.* Lymphotoxin pathway directs thymic Aire expression. *Nat Immunol* **4**, 1121-1127 (2003).
8. Venanzi, E.S., Gray, D.H., Benoist, C. & Mathis, D. Lymphotoxin pathway and Aire influences on thymic medullary epithelial cells are unconnected. *J Immunol* **179**, 5693-5700 (2007).
9. Martins, V.C., Boehm, T. & Bleul, C.C. Ltbetar signaling does not regulate Aire-dependent transcripts in medullary thymic epithelial cells. *J Immunol* **181**, 400-407 (2008).
10. Rennert, P.D., Browning, J.L., Mebius, R., Mackay, F. & Hochman, P.S. Surface lymphotoxin alpha/beta complex is required for the development of peripheral lymphoid organs. *J Exp Med* **184**, 1999-2006 (1996).
11. Lorenz, R.G., Chaplin, D.D., McDonald, K.G., McDonough, J.S. & Newberry, R.D. Isolated lymphoid follicle formation is inducible and dependent upon lymphotoxin-sufficient B lymphocytes, lymphotoxin beta receptor, and TNF receptor I function. *J Immunol* **170**, 5475-5482 (2003).
12. Bouskra, D.*, et al.* Lymphoid tissue genesis induced by commensals through NOD1 regulates intestinal homeostasis. *Nature* **456**, 507-510 (2008).
13. Vivier, E., Spits, H. & Cupedo, T. Interleukin-22-producing innate immune cells: new players in mucosal immunity and tissue repair? *Nat Rev Immunol* **9**, 229-234 (2009).
14. Ivanov, II*, et al.* Induction of intestinal Th17 cells by segmented filamentous bacteria. *Cell* **139**, 485-498 (2009).
15. Hsu, H.C.*, et al.* Interleukin 17-producing T helper cells and interleukin 17 orchestrate autoreactive germinal center development in autoimmune BXD2 mice. *Nat Immunol* **9**, 166-175 (2008).
16. Eberl, G. From induced to programmed lymphoid tissues: the long road to preempt pathogens. *Trends Immunol* **28**, 423-428 (2007).
17. Umesaki, Y., Setoyama, H., Matsumoto, S., Imaoka, A. & Itoh, K. Differential roles of segmented filamentous bacteria and clostridia in development of the intestinal immune system. *Infect Immun* **67**, 3504-3511 (1999).
18. Jiang, H.Q., Bos, N.A. & Cebra, J.J. Timing, localization, and persistence of colonization by segmented filamentous bacteria in the neonatal mouse gut depend on immune status of mothers and pups. *Infect Immun* **69**, 3611-3617 (2001).

19. De Togni, P.*, et al.* Abnormal development of peripheral lymphoid organs in mice deficient in lymphotoxin. *Science* **264**, 703-707 (1994).
20. Futterer, A., Mink, K., Luz, A., Kosco-Vilbois, M.H. & Pfeffer, K. The lymphotoxin beta receptor controls organogenesis and affinity maturation in peripheral lymphoid tissues. *Immunity* **9**, 59-70 (1998).
21. Scheu, S.*, et al.* Targeted disruption of LIGHT causes defects in costimulatory T cell activation and reveals cooperation with lymphotoxin beta in mesenteric lymph node genesis. *J Exp Med* **195**, 1613-1624 (2002).
22. Dear, T.N.*, et al.* The Hox11 gene is essential for cell survival during spleen development. *Development* **121**, 2909-2915 (1995).
23. Ye, P.*, et al.* Requirement of interleukin 17 receptor signaling for lung CXC chemokine and granulocyte colony-stimulating factor expression, neutrophil recruitment, and host defense. *J Exp Med* **194**, 519-527 (2001).
24. Tumanov, A.*, et al.* Distinct role of surface lymphotoxin expressed by B cells in the organization of secondary lymphoid tissues. *Immunity* **17**, 239-250 (2002).
25. Ramirez, A.*, et al.* A keratin K5Cre transgenic line appropriate for tissue-specific or generalized Cre-mediated recombination. *Genesis* **39**, 52-57 (2004).
26. Lee, P.P.*, et al.* A critical role for Dnmt1 and DNA methylation in T cell development, function, and survival. *Immunity* **15**, 763-774 (2001).
27. Hobeika, E.*, et al.* Testing gene function early in the B cell lineage in mb1-cre mice. *Proc Natl Acad Sci U S A* **103**, 13789-13794 (2006).
28. Lochner, M.*, et al.* In vivo equilibrium of proinflammatory IL-17+ and regulatory IL-10+ Foxp3+ RORgamma t+ T cells. *J Exp Med* **205**, 1381-1393 (2008).
29. Lee, P.Y.*, et al.* TLR7-dependent and FcgammaR-independent production of type I interferon in experimental mouse lupus. *J Exp Med* **205**, 2995-3006 (2008).
30. Hoffman, I.E.*, et al.* Specific antinuclear antibodies are associated with clinical features in systemic lupus erythematosus. *Ann Rheum Dis* **63**, 1155-1158 (2004).
31. De Rycke, L.*, et al.* Rheumatoid factor and anticitrullinated protein antibodies in rheumatoid arthritis: diagnostic value, associations with radiological progression rate, and extra-articular manifestations. *Ann Rheum Dis* **63**, 1587-1593 (2004).
32. Van Praet, L.*, et al.* Microscopic gut inflammation in axial spondyloarthritis: a multiparametric predictive model. *Ann Rheum Dis* **72**, 414-417 (2013).
33. Keeton, M., Ahn, C., Eguchi, Y., Burlingame, R. & Loskutoff, D.J. Expression of type 1 plasminogen activator inhibitor in renal tissue in murine lupus nephritis. *Kidney Int* **47**, 148-157 (1995).
34. Van der Sluis, M.*, et al.* Muc2-deficient mice spontaneously develop colitis, indicating that MUC2 is critical for colonic protection. *Gastroenterology* **131**, 117-129 (2006).
35. Franki, A.S.*, et al.* A unique lymphotoxin {alpha}beta-dependent pathway regulates thymic emigration of V{alpha}14 invariant natural killer T cells. *Proc Natl Acad Sci U S A* **103**, 9160-9165 (2006).
36. Boon, N., Top, E.M., Verstraete, W. & Siciliano, S.D. Bioaugmentation as a tool to protect the structure and function of an activated-sludge microbial community against a 3-chloroaniline shock load. *Appl Environ Microbiol* **69**, 1511-1520 (2003).
37. Muyzer, G., de Waal, E.C. & Uitterlinden, A.G. Profiling of complex microbial populations by denaturing gradient gel electrophoresis analysis of polymerase chain reaction-amplified genes coding for 16S rRNA. *Appl Environ Microbiol* **59**, 695-700 (1993).

38. Barman, M., *et al.* Enteric salmonellosis disrupts the microbial ecology of the murine gastrointestinal tract. *Infect Immun* **76**, 907-915 (2008).

Figure legends

Figure 1 Systemic autoimmune responses in mice lacking secondary lymphoid organs

(a) 3-month-old wild-type (C57BL/6), *Ltbr*$^{-/-}$, *Lta*$^{-/-}$, *LIGHT*$^{-/-}$ and *Ltbr*$^{-/-}$*Hox11*$^{-/-}$ mice; percentage of mice with at least one anti-ENA reactivity. (b) 6-months-old *Ltbr*$^{-/-}$ mice (n=15); percentage of mice with reactivity against a specific ENA. (c) LIA of 6-month-old *Ltbr*$^{-/-}$ mice; wild-type mice and 3-month-old Rorγt-*Ltb*$^{-/-}$ mice. (d) LTβR-Fc or control immunoglobulin (Ig) treated wild-type mice; percentage of mice with at least one anti-ENA reactivity. E denotes gestational day. *Anti-ENA were determined with LIA at the age of 3 months. **Anti-ENA were determined with LIA 12 weeks after the start of treatment. (e) 3-month-old cell-specific LT knock-out mice; percentage of mice with at least one anti-ENA reactivity. (f) Bone marrow cells from wild-type or *Ltbr*$^{-/-}$ mice were transferred at neonatal age into lethally-irradiated wild-type or *Ltbr*$^{-/-}$ mice; percentage of mice with at least one anti-ENA reactivity. Anti-ENA were determined with LIA at the age of 3 months.

Figure 2 Development of antinuclear antibodies in lymphotoxin deficient mice is influenced by gut microbiota

(a) *Ltbr*$^{-/-}$ mice were treated or not with antibiotics from birth (upper panel), conventionalized or germ free wild-type mice were treated with the LTβR-Fc fusion protein from gestational day 18 until six weeks after birth (lower panel); percentage of mice with at least one anti-ENA reactivity. Anti-ENA were tested with LIA at the age of three months. (b) Cluster analysis of denaturing gradient gel electrophoresis of luminal samples of wild-type, anti-ENA positive and anti-ENA negative *Ltbr*$^{-/-}$ mice. (c) Real-time PCR for SFB in luminal, mucosal and faecal samples of multiple anti-ENA positive and anti-ENA negative *Ltbr*$^{-/-}$ mice. Analysis with ANOVA, p=0.02 for differences between groups, n = 4 mice per group. Data represent means±s.e.m. (d) LTβR-Fc treated wild-type or *IL17R*$^{-/-}$ mice; percentage of mice with at least one anti-ENA reactivity. E denotes gestational day. Anti-ENA were determined with LIA at the age of 3 months.

Figure 3 Reduced IgA levels in mice and humans positive for antinuclear antibodies

(a) Serum IgA levels of multiple anti-ENA positive and anti-ENA negative *Ltbr*$^{-/-}$ mice, and *RAG2*$^{-/-}$ mice (negative control). Analysis with student's t-test, n = 6-22 mice per group. Data represent means±s.e.m. (b-c) Serum IgA and IgG levels of patients with systemic lupus erythematosus (SLE), rheumatoid arthritis (RA) and spondyloarthritis (SpA). Analysis with ANOVA with Bonferroni *post-hoc* tests: ***$P < 0.001$, NS, not significant ($P > 0.05$), n = 53-65 patients per group. Data represent means±s.e.m.

Figure 1

a

Strain	Anti-ENA
Wild-type	0/20 (0%)
Ltbr$^{-/-}$	4/17 (24%)
Ltb$^{-/-}$	4/15 (27%)
Lta$^{-/-}$	3/12 (25%)
LIGHT$^{-/-}$	0/10 (0%)
Ltbr$^{-/-}$*Hox11*$^{-/-}$	3/22 (14%)

b

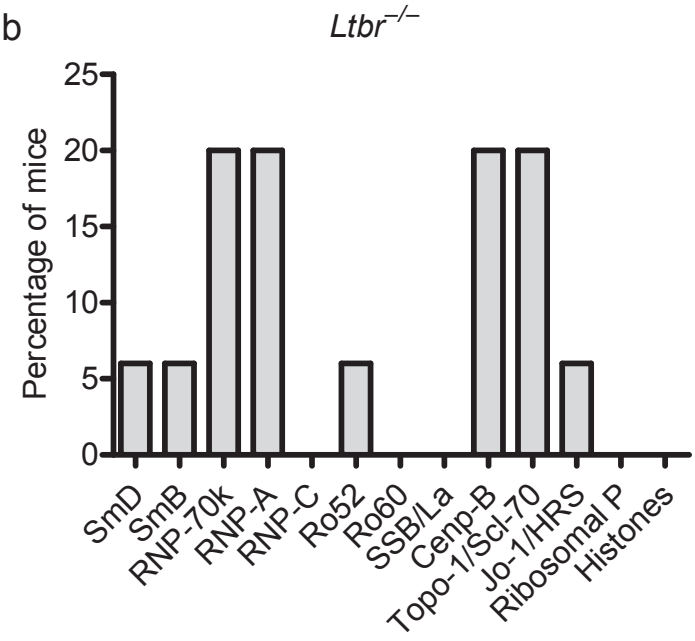

c

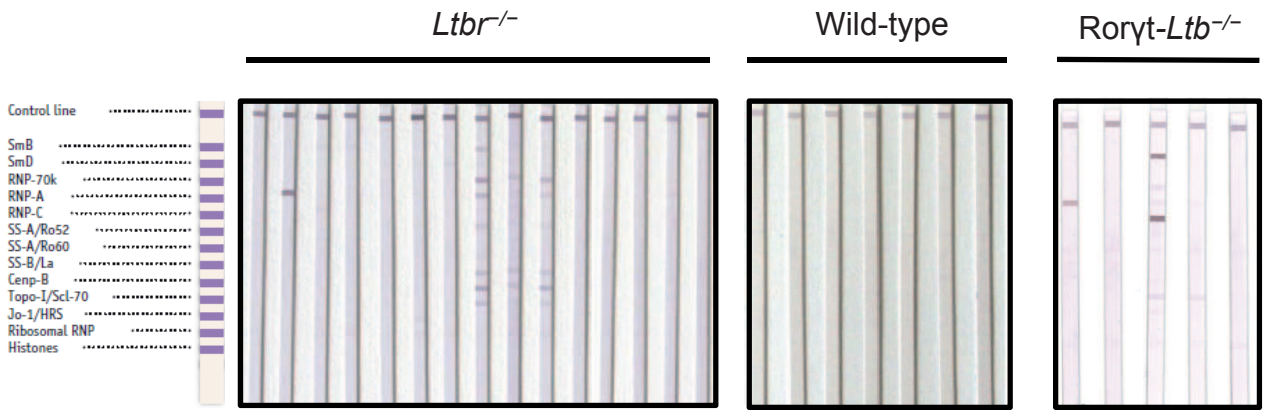

d

Reagent	Scheme	Litters (#)	Total progeny (#)	Anti-ENA
LTβR-Fc	E11 and E15	3	12	0/12*
LTβR-Fc	E18, once weekly until week 7	2	13	5/13*
Control Ig	E18, once weekly until week 7	2	13	0/13*
LTβR-Fc	Week 8, once weekly until week 15	-	8	0/8**

e

Strain	Anti-ENA
T-*Ltb*$^{-/-}$	0/10 (0%)
T-*Ltb*$^{+/+}$	0/7 (0%)
B-*Ltb*$^{-/-}$	0/7 (0%)
B-*Ltb*$^{+/+}$	0/2 (0%)
Roryt-*Ltb*$^{-/-}$	5/15 (33%)
Roryt-*Ltb*$^{+/+}$	0/11 (0%)

f

Strain	Anti-ENA
Wild-type→Wild-type	0/13 (0%)
Wild-type→*Ltbr*$^{-/-}$	5/21 (24%)
Ltbr$^{-/-}$→Wild-type	7/23 (30%)
Ltbr$^{-/-}$→*Ltbr*$^{-/-}$	5/21 (24%)

Figure 2

a

Strain	Anti-ENA
Untreated *Ltbr*$^{-/-}$	8/32 (25%)
Antibiotic treated *Ltbr*$^{-/-}$	4/32 (12%)
Conventionalised LTβR-Fc treated wild-type	6/15 (40%)
Germfree LTβR-Fc treated wild-type	3/13 (23%)

b

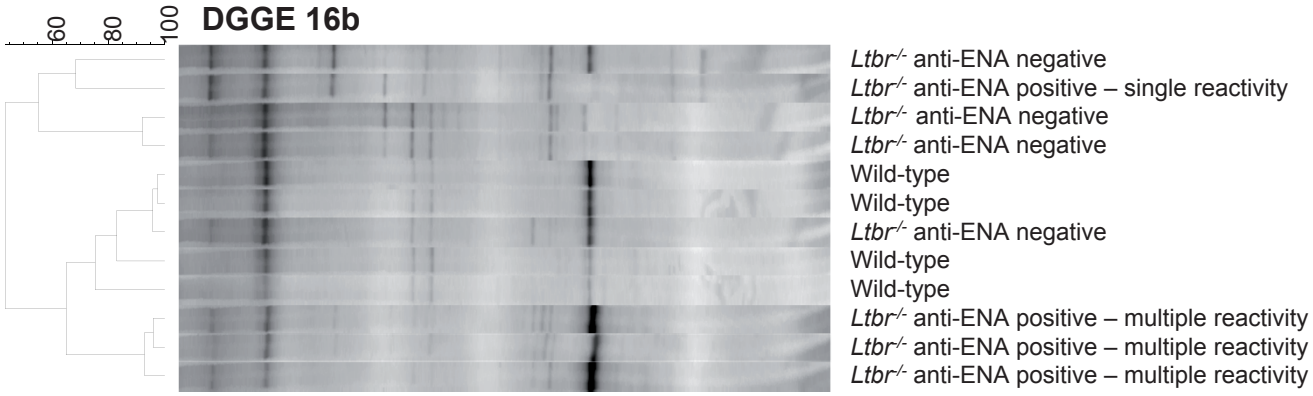

c

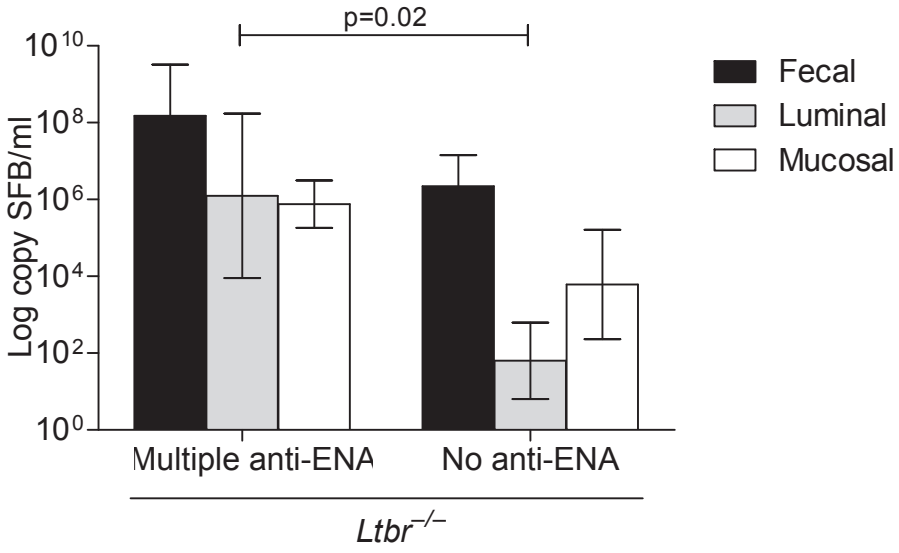

d

Strain	Scheme	Litters (#)	Total progeny (#)	Anti-ENA
Wild-type	LTβR-Fc E18, once weekly until week 7	2	13	5/13
IL-17R$^{-/-}$	LTβR-Fc E18, once weekly until week 7	2	13	1/13

Figure 3

a

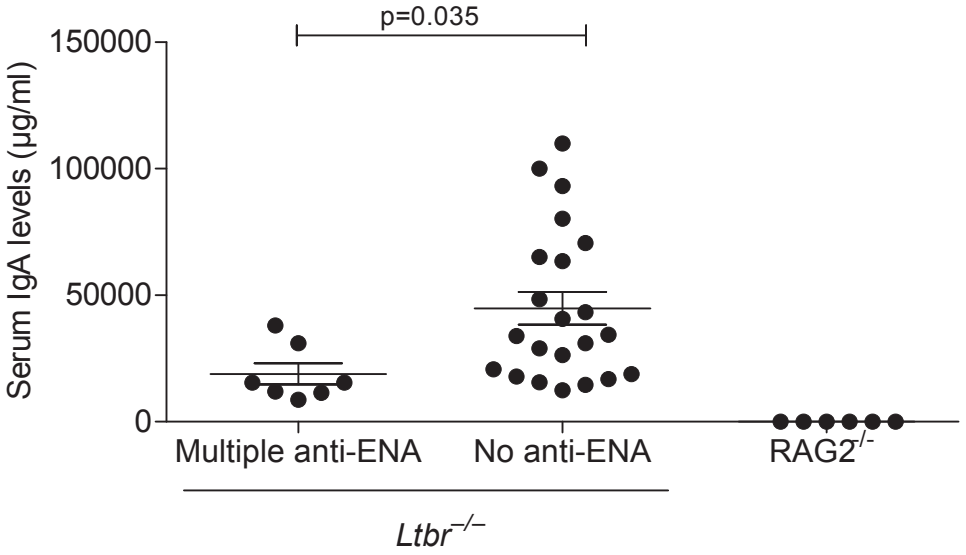
p=0.035
150000
100000
50000
0
Serum IgA levels (µg/ml)
Multiple anti-ENA
No anti-ENA
RAG2-/-
Ltbr–/–

b

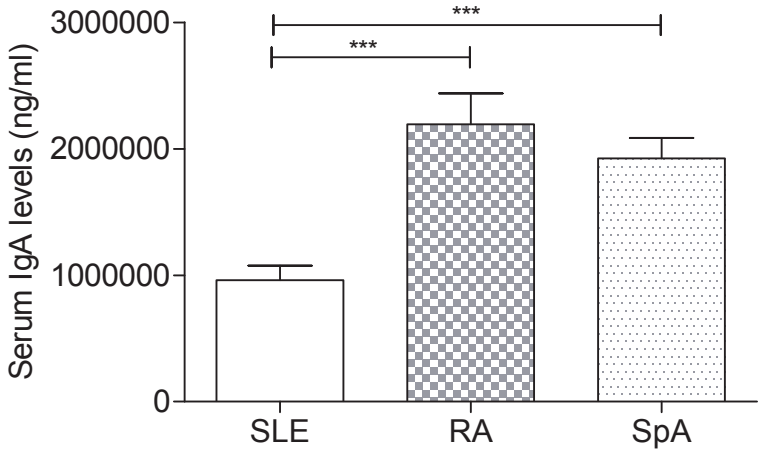
***
***
3000000
2000000
1000000
0
Serum IgA levels (ng/ml)
SLE
RA
SpA

c

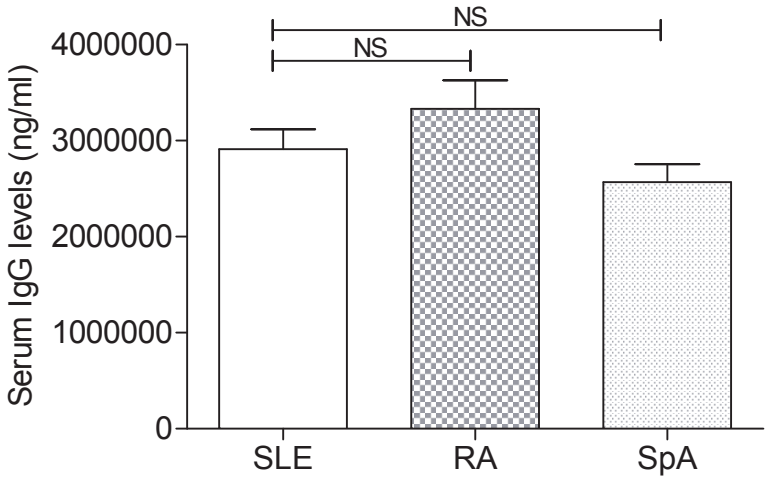
NS
NS
4000000
3000000
2000000
1000000
0
Serum IgG levels (ng/ml)
SLE
RA
SpA

Supplementary figure legends

Supplementary figure 1 Validation of sensitivity of line immunoassay for mouse anti-extractable nuclear antigen

(a) 16-week-old MRL/*lpr*$^{-/-}$ mice (n = 20); percentage of mice with reactivity against a specific ENA. (b) 24-week-old (NZW/NZB)F1 mice (n = 16); percentage of mice with reactivity against a specific ENA. (c) Pristane-induced lupus in C57BL/6 mice (n = 10); analysis after 24 weeks, percentage of mice with reactivity against a specific ENA. (d) 24-week-old NOD mice (n = 21); percentage of mice with reactivity against a specific ENA.

Supplementary figure 2 Absence of anti-dsDNA in *Ltbr*$^{-/-}$ mice

Anti-dsDNA IgG levels in 3-month-old wild-type (C57BL/6) and *Ltbr*$^{-/-}$ mice. 7-8 months (NZW/NZB) F1 were used as positive control. No significant difference was found between wild-type and *Ltbr*$^{-/-}$ mice, n = 5–8 mice per group. Data represent means±s.e.m.

Supplementary figure 3 Absence of specific autoimmune pathologic features in *Ltbr*$^{-/-}$ mice

(a) Representative images of interscapular skin (Masson trichrome, 20x magnification), esophagus (Masson trichrome, 100x magnification) and kidney (Periodic acid-Schiff, 400x magnification) of 12-month-old wild-type and *Ltbr*$^{-/-}$ mice are shown. (b) Histological scores of different organs of 12-month-old wild-type and *Ltbr*$^{-/-}$ mice. No significant differences were found, n = 7 – 11 per group. Data represent means±s.e.m.

Supplementary figure 4 LTβR expression in the thymic stroma is not required for anti-ENA development

(a) Thymic reconstitution was analyzed by counting total cell number and flow cytometry for cell percentages. Numbers represent the percentages within the indicated regions (left panel). No significant differences were found. Data represent means±s.e.m. (b) T cell reconstitution of spleen was assessed by flow cytometry. Numbers represent the percentages within the indicated regions. (c) Total IgG from nude mice engrafted with *Ltbr*$^{-/-}$ or wild-type thymi was determined by ELISA. No significant differences were found. Data represent means±s.e.m. (d) Sera were collected 12 weeks after transplantation and tested for anti-ENA; percentage of mice with at least one anti-ENA reactivity.

Supplementary figure 5 Histological analysis of the gut of anti-ENA positive and negative *Ltbr*$^{-/-}$ mice

(a) Inflammatory scores of different part of the gut of 3-months-old *Ltbr*$^{-/-}$ mice are shown. No significant differences were found, n = 4 per group. Data represent means±s.e.m. (b) Scoring scheme.

Supplementary figure 6 Histological analysis of the gut of anti-ENA positive and negative *Ltbr*$^{-/-}$ mice Representative images of different regions of the gut are shown (haematoxylin and eosin staining left, Periodic acid-Schiff staining right, electron microscopy bottom).

Supplementary Figure 1

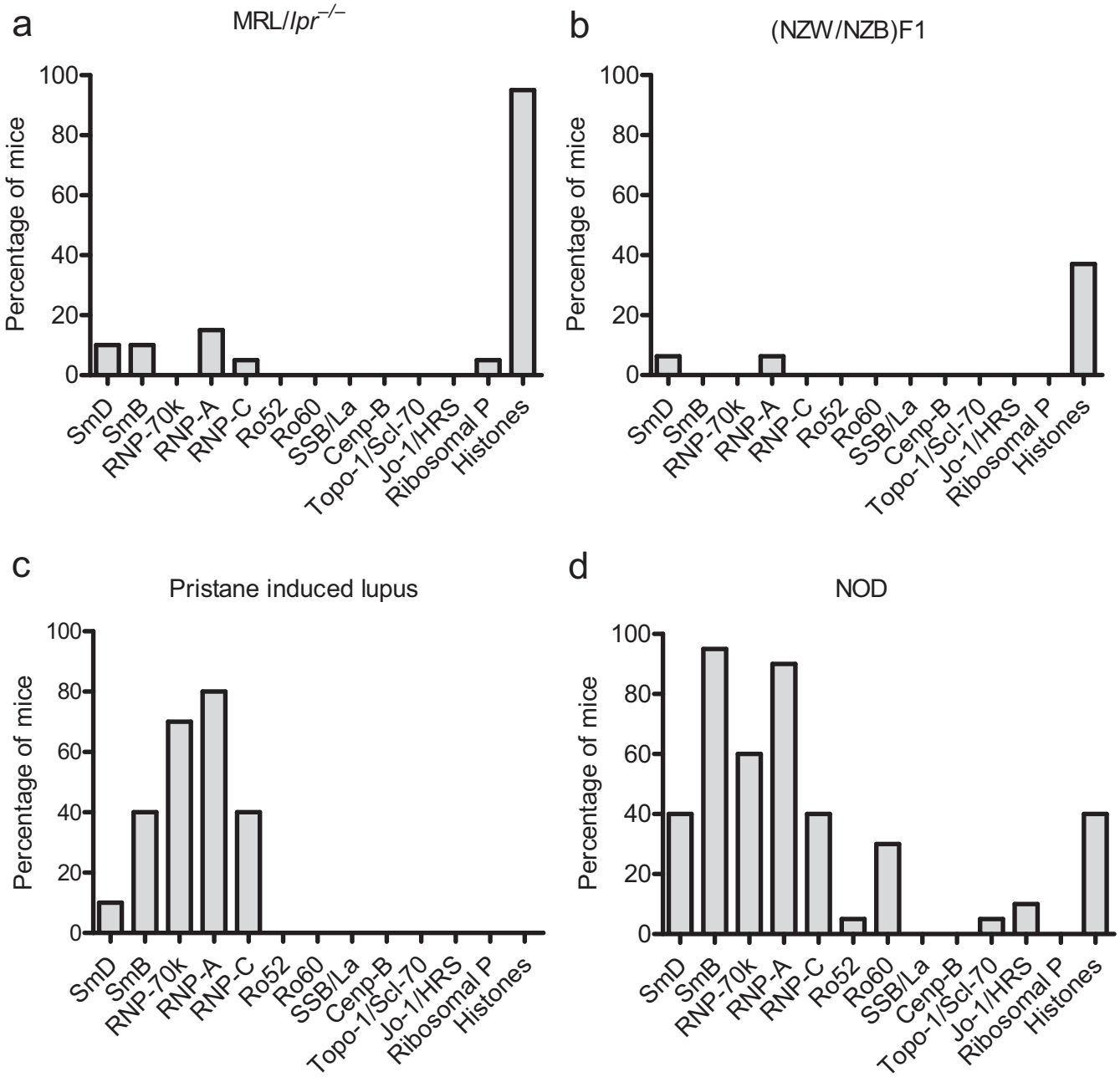

Supplementary Figure 2

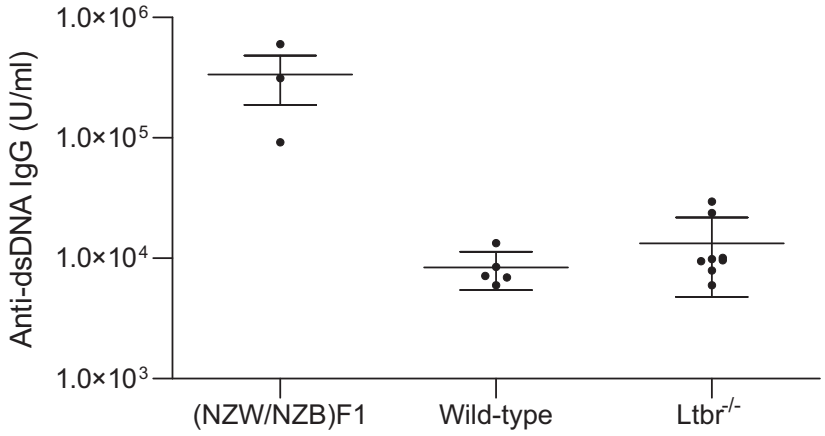

Supplementary Figure 3

a

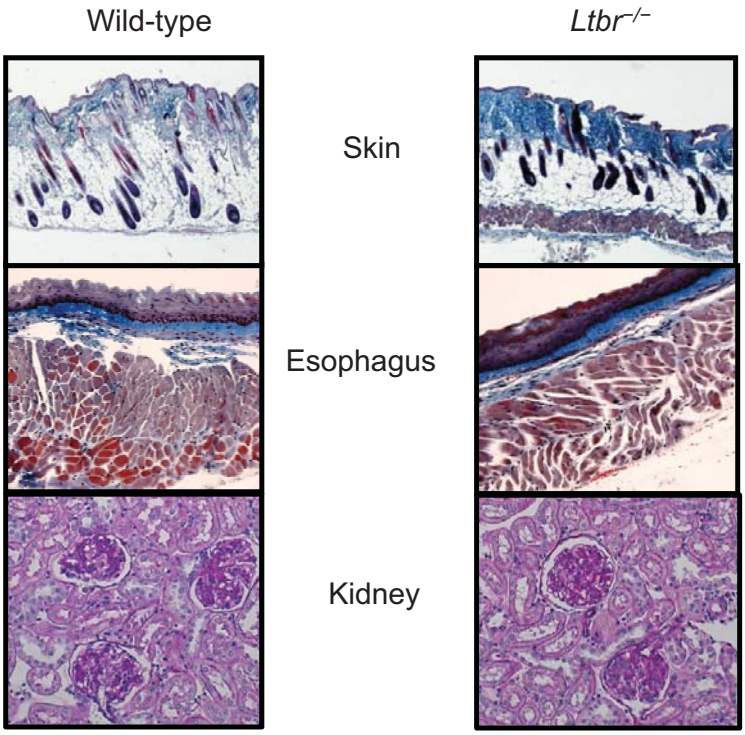

b

Scoring parameter	Wild-type	*Ltbr*$^{-/-}$
Kidney - Glomerular score	2.2±0.25	1.6±0.29
Kidney - Interstitial inflammation	1.1±0.23	0.91±0.28
Kidney - Glomeral crescents	0.1±0.1	0.18±0.18
Kidney - Vascular inflammation	0.2±0.2	0.09±0.09
Skin sclerosis	286±42	228±40
Esophagal sclerosis	39±2.0	29±4.6

Supplementary Figure 4

a

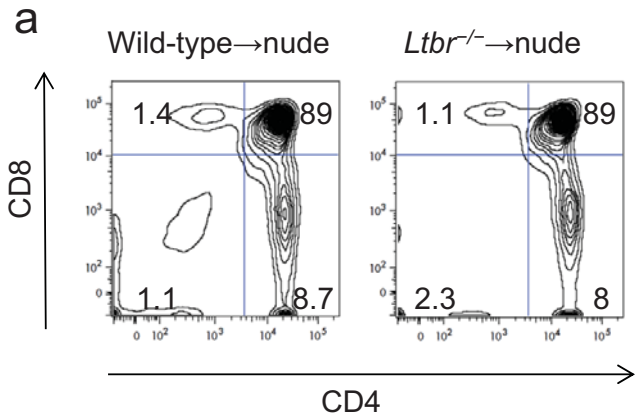

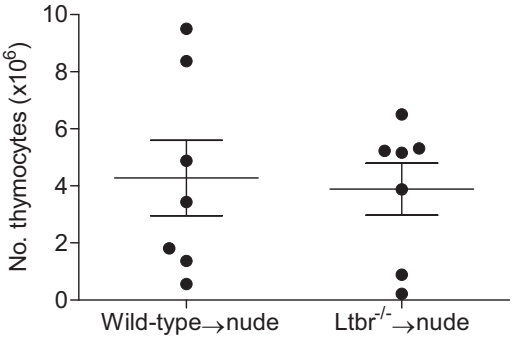

b

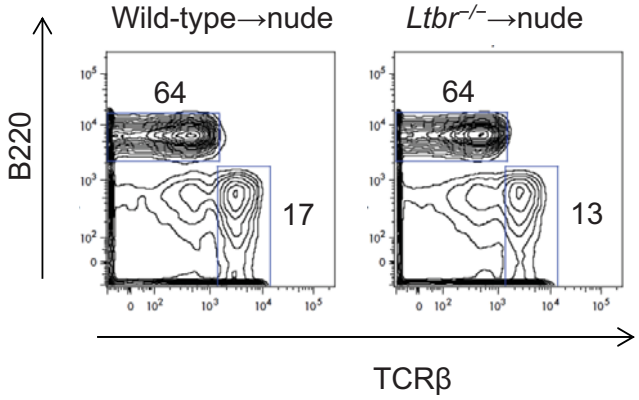

c

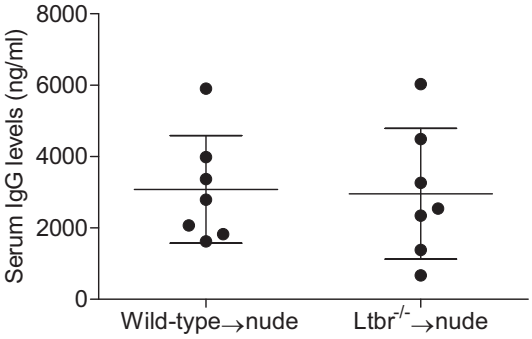

d

Strain	Anti-ENA
Wild-type→nude	0/7 (0%)
Ltbr$^{-/-}$→nude	0/7 (0%)

Supplementary Figure 5

a

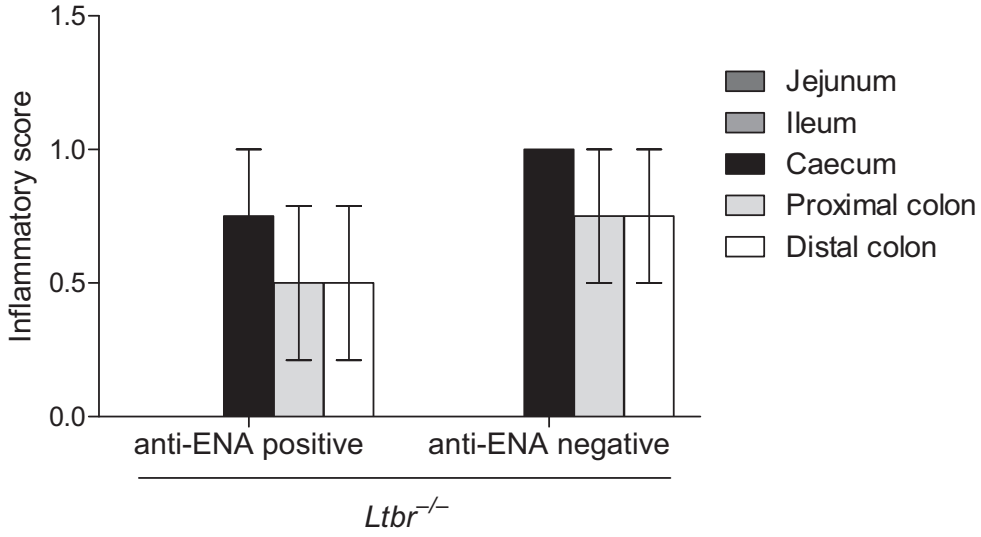

b

Histologic scoring scheme

	Score				
Criterion	0	1	2	3	4
Goblet cells	/	-	--	---	---
Mucosa thickening	/	+	++	+++	+++
Inflammatory cells	/	+	++	+++	+++
Submucosa cell infiltration	/	/	+	++	+++
Destruction of architecture	/	/	/	+	++
Ulcers (epithelial cell surface)	0%	0-25%	25-50%	50-75%	75-100%
Crypt abscesses	0	1-3	4-6	7-9	>10

Supplementary Figure 6